JACS
JOURNAL OF THE AMERICAN CHEMICAL SOCIETY
Article
pubs.acs.org/JACS

The Origin of the Odd–Even Effect in the Tunneling Rates across EGaIn Junctions with Self-Assembled Monolayers (SAMs) of *n*-Alkanethiolates

Li Jiang,[†] C. S. Suchand Sangeeth,[†] and Christian A. Nijhuis*[,†,‡,§]

[†]Department of Chemistry, National University of Singapore, 3 Science Drive 3, Singapore 117543, Singapore

[‡]Solar Energy Research Institute of Singapore (SERIS), National University of Singapore, 7 Engineering Drive 1, Singapore 117574, Singapore

[§]Centre for Advanced 2D Materials and Graphene Research Centre, National University of Singapore, 6 Science Drive 2, Singapore 117546, Singapore

Supporting Information

ABSTRACT: Odd–even effects in molecular junctions with self-assembled monolayers (SAMs) of *n*-alkanethiolates have been rarely observed. It is challenging to pinpoint the origin of odd–even effects and address the following question: are the odd–even effects an interface effect, caused by the intrinsic properties of the SAMs, or a combination of both? This paper describes the odd–even effects in SAM-based tunnel junctions of the form $Ag^{A\text{-}TS}$-SC_n//GaO_x/EGaIn junctions with a large range of molecular lengths (n = 2 to 18) that are characterized by both AC and DC methods along with a detailed statistical analysis of the data. This combination of techniques allowed us to separate interface effects from the contributions of the SAMs and to show that the odd–even effect observed in the value of J obtained by DC-methods are caused by the intrinsic properties of the SAMs. Impedance spectroscopy (an AC technique) allowed us to analyze the SAM resistance (R_{SAM}), SAM capacitance (C_{SAM}), and contact resistance, within the junctions separately. We found clear odd–even effects in the values of both R_{SAM} and C_{SAM}, but the odd–even effect in contact resistance is very weak (and not responsible for the observed odd–even effect in the current densities obtained by J(V) measurements). Therefore, the odd–even effects in $Ag^{A\text{-}TS}$-SC_n//GaO_x/EGaIn junctions are attributed to the properties of the SAMs and SAM–electrode interactions which both determine the shape of the tunneling barrier.

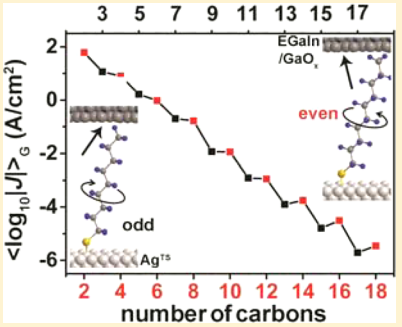

INTRODUCTION

Controlling and understanding charge transport at the nanoscale via chemical modification of interfaces is important in disciplines ranging from electrochemistry,[1−4] catalysis,[5,6] biochemistry,[7,8] to nanoelectronics.[9−11] One of the objectives of molecular electronics is to control the flow of charges across electrode—molecule—electrode structures (which consist of either a single molecule or a self-assembled monolayer; SAM) by modification of the chemical and supramolecular structure of the molecular component.[12−23] Physical–organic studies of charge transport are still difficult to perform, especially in two-terminal junctions, because usually only the total current response is measured as a function of applied bias. Such J(V) measurements do not make it possible to separate the contributions from the molecule–electrode interfaces and the molecular component from each other in a straightforward manner.[17,24−30]

An attractive method to study how the electrical properties of the junctions depend on subtle changes in the SAM structure is to study so-called "odd–even" effects.[2,23,31−34] Here only the number of a repeat unit of the molecular structure is changed while leaving all other components of the junction (the electrode materials and the nature of SAM—electrode contacts) unchanged. We, and others, studied odd–even effects in SAM-based junctions with SAMs of the form $S(CH_2)_{n-1}CH_3$ (for short, SC_n),[32,34] and SAMs in which the terminal CH_3 group was replaced by a ferrocenyl (Fc)[33] or phenyl (Ph)[23] moiety. In these examples the number of CH_2 units (i.e., the value of n) was changed. The odd–even effects in junctions with SAMs with Fc (with Ag bottom electrodes and EGaIn top electrodes; see below) or Ph (with Si bottom electrodes and Pb top electrodes) were related to the odd–even effect in the tilt angle of the terminal group, which, in turn, impacted the rectification ratio of a molecular diode or the tunneling barrier height, respectively. The origin of the odd–even effects in junctions with SC_n SAMs (so far only studied in junctions with Ag or Au bottom electrodes and EGaIn top contacts) remains unclear.[32,34]

In this work we address the following question: is the odd–even effect a molecular effect, an interface effect, or a combination of both, in junctions of the form $Ag^{A\text{-}TS}$-SC_n/GaO_x/EGaIn (Figure 1)? Previous studies relied solely on J(V) measurements where J is the total current (in A/cm^2) that flows

Received: June 3, 2015
Published: July 31, 2015

DOI: 10.1021/jacs.5b05761
J. Am. Chem. Soc. 2015, 137, 10659−10667

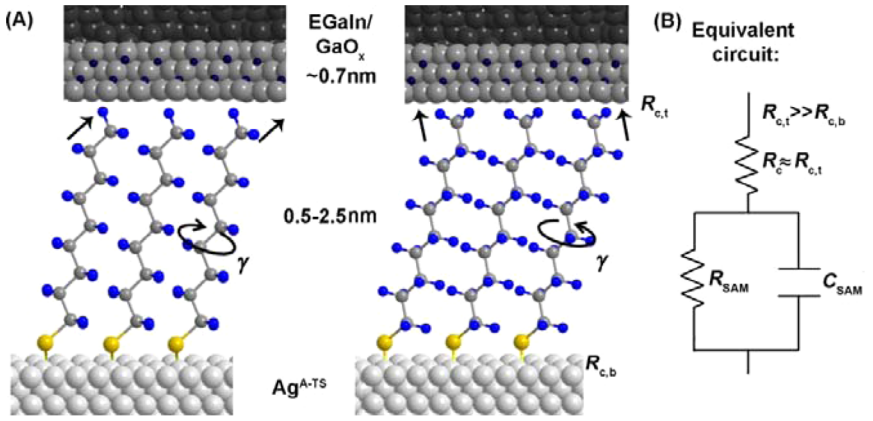

Figure 1. Schematic illustrations of odd-numbered and even-numbered *n*-alkanethiolate SAM based junction (A) and the equivalent circuit for these junctions (B). The arrows indicate the odd−even effect in the orientation of the terminal CH_3 moiety. The GaO_x/EGaIn is a noninvasive top electrode based on a liquid-metal alloy of eutectic Ga and In passivated with a highly conductive 0.7 nm thick layer of GaO_x.[29,44,45] The γ is the chain twist angle of the molecule, and odds and evens have opposite signs as indicated by the arrows[46] (for clarity, we kept the sign of the tilt angle of the SAM fixed and defined γ with respect to this tilt angle). The SAM-top contact resistance ($R_{c,t}$) is roughly 2 orders of magnitude larger than the SAM-bottom contact resistance ($R_{c,b}$), so the contact resistance (R_c) is dominated by the SAM-top contact resistance ($R_{c,t}$).

across the junction as a function of bias V. The value of J (which is impeded by all components of the junction) is usually interpreted using a simple tunnel equation (eq 1) where J_0 (in A/cm^2) is a pre-exponential factor, d (in units of n_C) is the thickness of the SAM, and β (in n_C^{-1}) is the tunneling decay coefficient. However, this approach does not make it possible to separate molecular effects from interface effects, and the physical meaning of the values of both J_0 (often associated with the contact resistance) and β (often related to the shape/height of the tunneling barrier) is unclear.[35,36]

$$J = J_0 e^{-\beta d} \tag{1}$$

The electrical response of a junction is affected by the properties of the SAM, the top and bottom electrodes, a protective layer (if present), and the SAM−electrode interfaces.[12,29,33,37−43] Figure 1 shows a schematic of the Ag^{TS}-SC_n//GaO_x/EGaIn junction along with the equivalent circuit of that junction. As indicated, it is expected that the orientation of the terminal CH_3 group with respect to the top electrode follows an odd−even effect resulting in an odd−even effect in SAM—top electrode interaction. Initial studies hypothesized that (i) if this odd−even effect in the orientation of the CH_3 terminal group results in an odd−even effect in the contact resistance, it would cause an odd−even effect in the value of J_0 and (ii) if this odd−even effect in the orientation of the CH_3 terminal group results in an odd−even effect in the shape of the tunneling barrier, it would cause an odd−even effect in the value of β.[32,34]

Thuo et al.[32] reported that the tunneling rates across junctions of the form Ag^{TS}-SC_n//GaO_x/EGaIn (n = 9−18) follow odd−even effects (where Ag^{TS} is a template-stripped Ag electrode[47]). A rigorous statistical analysis concluded that both J_0 and β contribute to the odd−even effect or, in other words, both the interfaces and the SAM contribute to the odd−even effect.[48] Baghbanzadeh et al.[34] followed-up on the study by Thuo et al. using a broad range of values of n = 5−18. Remarkably, in this study the odd−even effects of junctions with Ag^{TS} electrodes could not be reproduced which may have been caused by a change in the fabrication method of the EGaIn tip and formation of the junctions (the authors used "flattened" tips and large junction sizes;[49] how these changes in the tip and contact formation affect the junctions are not clear). The authors concluded that the odd−even effect is caused by the SAM//GaO_x interfaces in junctions with Au^{TS} electrodes based on an odd−even effect in the value of J_0 and the absence of an odd−even effect in the value of β. More precisely, the authors suggested the odd−even effect effectively changes the SAM//GaO_x interface.

Recently we reported how impedance spectroscopy can be used to measure the contribution of each component that impedes charge transfer directly (i.e., separate interface effects from molecular effects) using the equivalent circuit shown in Figure 1B.[29] In these junctions the native GaO_x layer does not impede charge transfer significantly and assuming that $R_c = R_{c,t}$ ($R_{c,t}$ is the contact resistance of the noncovalent SAM—top electrode contact) only introduces an error of ∼2% in the analysis of the data. To address the question of whether the odd−even effect is an interface or a molecular effect (see for definitions in the Background section), we determined the contribution of the molecule—electrode contact resistance (R_c), and the resistance (R_{SAM}) and capacitance (C_{SAM}) of the SAMs, directly with impedance spectroscopy.

Here, we used top electrodes of GaO_x/EGaIn stabilized in a fluidic device made of PDMS (polydimethylsiloxane)[50] and cone-shaped GaO_x/EGaIn tips to form contacts to SC_n SAMs on Ag^{A-TS} and characterized the junctions by both DC and AC methods. (The Ag^{A-TS} surfaces were prepared using an annealing step before template-stripping to remove small grains to yield ultrasmooth Ag surfaces that only consist of large grains and therefore have only a small fraction of exposed grain boundaries.[26,51]) To minimize the error associated with the extrapolation of the DC data to n = 0, we used a large range of n values (n = 2−18). To rule out uncertainties in the preparation and formation of the top contacts, we used two types of EGaIn electrodes. We found that the odd−even effect in the value of J obtained by DC methods originates from an odd−even effect in the SAM resistance (R_{SAM}) and that the SAM—electrode contact resistance (R_c) only contributes marginally (too small to be measurable by DC methods) to the device characteristics. The value of R_{SAM} depends on both the SAM—electrode interaction and the SAM packing which determine the tunneling barrier height. Thus, both "molecular

DOI: 10.1021/jacs.5b05761
J. Am. Chem. Soc. 2015, 137, 10659−10667

effects" and "interface effects" (see Background for definitions) determine the shape of the tunneling barrier but the contact resistance (as defined below in eq 2) does not affect J(V) measurements. Interestingly, the odd−even effect in the capacitance (C_{SAM}) of the SAMs is remarkably large which suggests that SAMs are promising candidates for high-performance dielectrics.[52−56]

BACKGROUND

Molecular vs Interface Effects. Although the terms "molecular effects" and "interface effects" have been frequently used in the context of SAM-based junctions to pinpoint which part of the junction dominates the electrical characteristics of the junctions, these terms are usually not well-defined. From a theoretical point of view such a distinction is not straightforward, and why that is can be easily explained using the Landauer formalism for instance. Equation 2 shows the conductance across a two-terminal junction for coherent tunneling assuming ohmic molecule—metal contacts where h = Planck's constant, e = the charge of an electron, T = the transmission probability, and M = the number of conduction channels (the transverse modes).[57] For the case of an ideal point contact, the contact resistance is the inverse of the universal quantum conductance G_0 (= $2e^2/h$ for M = 1). In eq 2 G_C denotes the resistance at the molecule−electrode interface which does not depend on T (even when T = 1, as is the case for a ballistic conductor, the resistance across the junction will be $1/G_0$). In EGaIn junctions the contacts are unlikely to be ideal point contacts[49] and hence we expect G_C to be $\ll G_0$. The G_{SAM} denotes the conductance from one lead to the other which depends on T which is the probability for an electron to traverse the "conductor"—the reflection is given by $(1 - T)$.

$$G_{junction} = \frac{2e^2M}{h} + \frac{2e^2M}{h}\frac{T}{1-T} = G_C + G_{SAM} \quad (2)$$

The values of T and M depend on many factors including the molecular properties of the SAM and the Fermi-level of the electrode materials, *and* the properties of the SAM—electrode contacts. The molecule−electrode coupling Γ is a contributing factor to the value of T. The value of Γ depends on the binding energy between the SAM and the electrodes (the metal−S bond or van der Waal contacts in our case) and on the intramolecular coupling between the electrodes and the molecular frontier orbital. Therefore, a large value of Γ indicates strong molecule−electrode coupling and Γ relates to T as given by the Breit−Wigner formula[57]

$$T(E) = \frac{\Gamma_L\Gamma_R}{(E - E_{ME})^2 + \frac{1}{4}(\Gamma_L + \Gamma_R)^2} \quad (3)$$

where E is the applied bias, E_{ME} is the energy of the molecular frontier orbital involved in conduction relative to the Fermi levels of the electrodes, and Γ_L and Γ_R are the coupling parameters of the molecules to the left and right electrodes, respectively. Hence, in this context one cannot distinguish between "molecular effects" and "interface effects", as both determine the shape of the tunneling barrier and observables including the value of β and J_0.

Usefulness of "β-Plots". A convenient method to describe the charge transport properties of junctions determined by two-terminal DC measurements is to measure J(V) curves as a function of molecular length and plotting J vs d for a given, usually low, bias to yield the so-called "β-plot". A fit to eq 1 yields the values of J_0 and β which are associated with the "molecule−electrode interface" and "the shape of the tunneling barrier", respectively. Such a distinction is not straightforward, as explained above, because *both* J_0 and β depend on T and M (eqs 2−3). In addition, in this simple "β-plot" analysis J_0 is also bias dependent complicating the interpretation, and comparison across test beds, of J_0 even more. Equation 1 relates to eq 2 as $T \propto e^{-\beta d}$. Therefore, eq 1 can be best seen as a general tunneling equation with J_0 simply being a convenient fitting parameter.

Discussing the values of J_0 is still useful because the value of J_0 can be easily determined and compared across different types of junctions by treating J_0 as an "effective contact resistance". Such comparisons help to explain the vast difference in electronic properties observed across different types of junctions for a given molecular system. For instance, we used the value of J_0 to guide discussions regarding the role of defects in junctions,[35] and Whitesides et al., to establish effective contact areas,[49] or to identify which kind of functional groups affect the tunneling rates.[13,58,59]

Experimental Studies of Odd−Even Effects in SAM-Based Junctions. Odd−even effects have been only rarely studied in molecular junctions. Besides junctions with SAMs of SC_n, large odd−even effects have been observed in two types of junctions with SAMs with large terminal groups.[23,33] In junctions of the form Ag^{TS}-SC_nFc//GaO_x/EGaIn the tilt angle of the Fc is 5° smaller for n_{odd} than n_{even}.[33] This small tilt angle resulted in small steric repulsions between the Fc groups and better packed SAMs than for those SAMs with large tilt angles. The SAMs that packed well were more robust during the fabrication of the top electrodes resulting in junctions with smaller leakage currents and higher rectification ratios (by a factor of 10) and thus higher yields in nonshorting junctions (of 10%) with higher reproducibility (by a factor of 3) than those junctions with n_{even}.[33] (In a separate study we will report how this odd−even effect influences the work function, surface dipole, and the tunneling barrier height.)[60] Cahen et al.[23] reported an odd−even effect in the tilt angle of 20° of the Ph group in junctions of the form Si−C_nPh//Pb. This difference in the tilt caused an odd−even effect in the π−π interactions between the molecules and consequently in the barrier height.

Theoretical Studies of Odd−Even Effects in SAM-Based Junctions. To the best of our knowledge, so far only two theoretical studies have been reported on odd−even effects in SAM-based junctions. Dubi[61] studied how molecule−molecule interactions in the SAM affect the charge transport properties across junctions and found that coupling of charge carriers to phonons associated with the SAM (resulting in a loss of phase/coherence) could cause an odd−even effect. In this mechanism, the magnitude of the odd−even effect depends on both coherent transport along the backbone of the molecule and incoherent transport between molecules.[61] The odd−even effect decreases with increasing value of n and offset energies between the molecular frontier orbitals and the Fermi levels of the electrodes.

Zhang et al.[62] offered an alternative explanation and suggested that an odd−even effect in the twist angle γ could be important (see Figure 1) in agreement with the experimental observation of a change of the sign of γ (i.e., clockwise vs counterclockwise orientation) reported by Laibinis et al.[46] Zhang et al. showed that the value of γ determines how the distal hydrogen interacts with the top electrode; this difference in the interaction results in an odd−even effect in the shape of

DOI: 10.1021/jacs.5b05761
J. Am. Chem. Soc. 2015, 137, 10659−10667

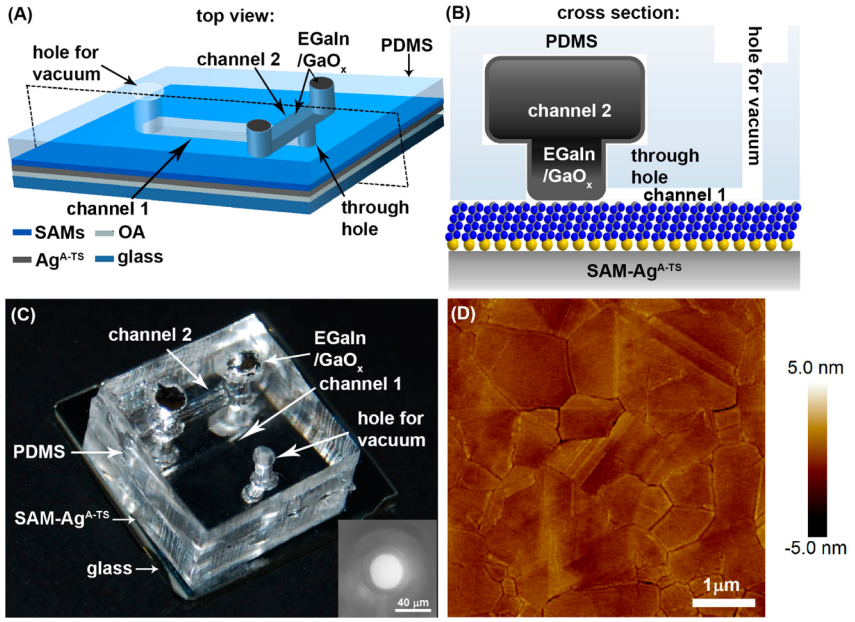

Figure 2. Schematic illustrations of the top (A) and side views (B) of the junctions. Channel 2 in the PDMS mold is filled with the EGaIn and is forced into the through-hole by applying a vacuum to channel 1. Channel 1 is small enough so that the EGaIn cannot fill it because of its high surface tension. The top electrode can be placed in contact with the SAM and removed again once the measurements are completed, and reused again for typically 20−25 times. (C) Photograph of a complete device. Inset shows an optical micrograph of the footprint of the GaO_x/EGaIn stabilized in the through-hole in contact with a transparent electrode (ITO) viewed through the ITO. (D) Atomic force microscopy (AFM) image of the template-stripped Ag surface ($Ag^{A\text{-}TS}$) that was annealed prior to template-stripping.

the tunneling barrier and, consequently, in the measured value of J. The authors noted that the odd−even effect manifested via this mechanism would be pronounced for $10 < n < 19$ (the regime of well-ordered solid-like SAMs).[62]

RESULTS AND DISCUSSION

Fabrication of the Junctions. We fabricated the junctions using a previously reported method (see Supporting Information for more details).[35,50] Figure 2 shows schematic illustrations and a photograph of the junctions. The GaO_x/EGaIn top electrode is stabilized in a through-hole in PDMS (polydimethylsiloxane) which is placed in contact with the SAMs immobilized on annealed template-stripped Ag ($Ag^{A\text{-}TS}$) bottom electrodes (the preparation of the $Ag^{A\text{-}TS}$ surfaces has been reported elsewhere[51]). Unlike template-stripped surfaces that have not been annealed prior to template-stripping, the $Ag^{A\text{-}TS}$ only consists of large grains because the annealing step effectively removes the small grains that are usually present between the large grains.[25,26] The atomic force micrograph (AFM; Figure 2D) shows that the surface $Ag^{A\text{-}TS}$ surface only consists of large grains (close to 1 μm^2 on average) and has a root-mean-square (rms) roughness of 0.6 nm over 5 × 5 μm^2. We note that we only used freshly template-stripped surfaces and purified the n-alkanethiols as previously described before we used them (see Supporting Information).

Here we used a geometrical junction area (A_{geo}) of 9.6×10^2 μm^2 because our previous study showed that the value of J scales with area when $A_{geo} \leq 9.6 \times 10^2$ μm^2 (indicating that leakage currents flowing across defects are not important),[35] but the A_{geo} is large enough so that the capacitance of the junctions can be reliably determined for junctions with a broad range of values of n = 6−18. The electrical characteristics for junctions with n = 2−5 were measured using cone-shaped tips[25,33,63,64] of GaO_x/EGaIn because this method gave a higher yield (60−90%) in nonshorting junctions than the method with the EGaIn stabilized in microchannels in this range of values of n. We do not know the reason for this difference in the yield in nonshorting junctions between the two methods at low values of n, but it seems that the approach speed of the top electrode to the SAMs, and contact formation with the SAMs, can be better controlled with the cone-shaped tip method than with the PDMS-stabilized EGaIn top electrodes.

***J*(V) Measurements.** We measured J(V) curves of n-alkanethiolate (n = 2−18) based SAMs over the bias range of ±0.5 V. We collected 300−350 J(V) curves (one curve includes trace and retrace) for each type of junction (see Table S1). The electrical characteristics (number of junctions, yields, and standard deviations) of the junctions are summarized in Table S1. The yield in stable junctions (junctions that did not short during the measurement or changed current abruptly by more than 2 orders of magnitude) was on average 81%, and for each type of junction we recorded 20 J(V) traces (300 in traces in total obtained from 15 junctions) on stable junctions. We plotted all values of J measured for each bias in histograms to which we fitted Gaussians to determine the Gaussian mean of the log-average of J ($\langle \log_{10}|J| \rangle_G$) and the log-standard deviation (σ_{log}). The details of this statistical analysis have been published before[48] (see Supporting Information for details).

Figure 3 shows the histograms of $\log_{10}|J|$ for an applied bias of −0.50 V with the Gaussian fits to these histograms. This was repeated for each applied bias, and from these Gaussian fits the $\langle \log_{10}|J| \rangle_G$ and σ_{log} were determined from which the log-average J(V) curves were constructed. Figure 3A and 3C show the log-average J(V) curves and indicate that the error bars (99% confidence levels) are not overlapping (the log-standard deviations (σ_{log}) were low and ranged from 0.12 to 0.57; Table S1). The statistically large numbers of J(V) data and the

DOI: 10.1021/jacs.5b05761
J. Am. Chem. Soc. 2015, 137, 10659−10667

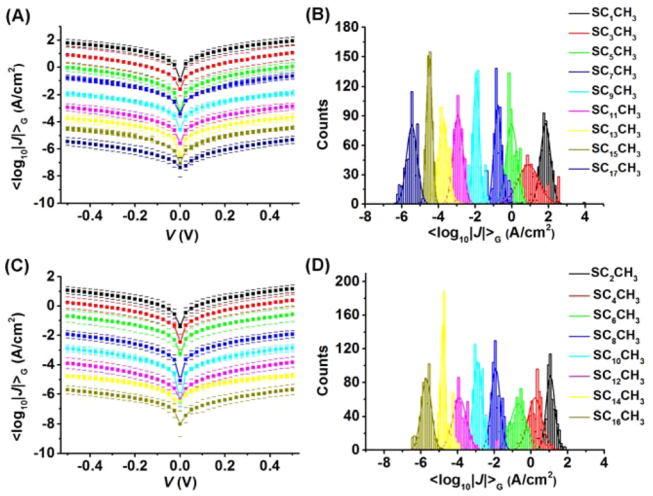

Figure 3. Plots of $\langle \log_{10}|J| \rangle_G$ vs applied bias for junctions with n_{even} (A) and n_{odd} (C). Histograms of $\log_{10}|J|$ at −0.50 V with Gaussian fits to these histograms for junctions with n_{even} (B) and n_{odd} (D).

small errors result in good 99% confidence levels in the log-average values of $\langle \log_{10}|J| \rangle_G$, $\log_{10}|J_0|$, and β.

The Odd Effect. Figure 4 shows the values of $\langle \log_{10}|J| \rangle_G$ determined at −0.50 V as a function of n for even-numbered (red) and odd-numbered (black) n-alkanethiolate based SAMs. We used two methods to extract the values of β and J_0 from the data: (i) by fitting eq 1 to a plot of $\langle \log_{10}|J| \rangle_G$ determined at

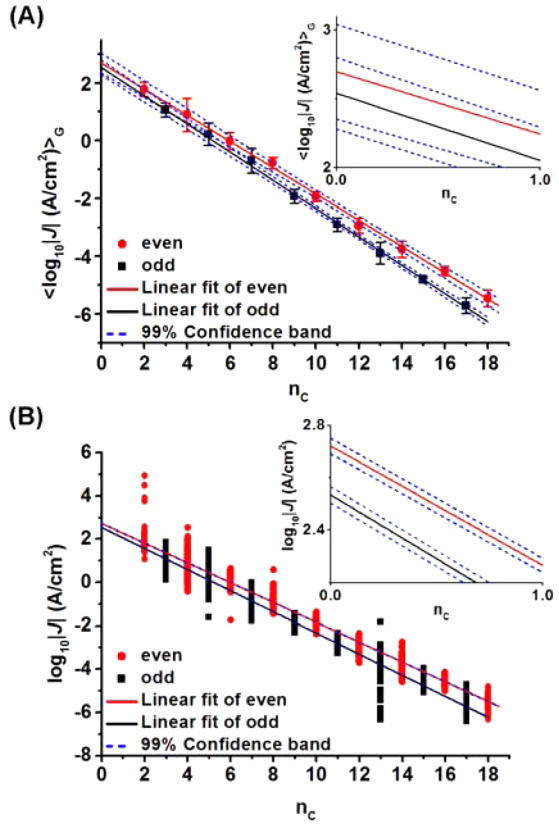

Figure 4. (A) The values of $\langle \log_{10}|J| \rangle_G$ (determined at −0.5 V) plotted against n with fits (solid lines) to eq 1 obtained using method 1 (as explained in the text) along with the 99% confidence levels. (B) All values of $\log_{10}|J|$ at −0.5 V with a fit to eq 1 obtained by method 2 (solid lines). Insets show the extrapolation to $n = 0$ in more detail.

−0.50 V as a function of n by minimizing the square of the errors and assuming that the data follow normal distributions (Figure 4A; method 1) or (ii) by fitting eq 1 to all data by minimizing the absolute values of the error (least absolute deviation fitting, LAD) without making any assumptions regarding the type of distribution the data follow (Figure 4B; method 2).[35,48,50] The magnified plots of the extrapolation of n back to 0 show that the 99% confidence bands overlap using method 1 (inset of Figure 4A), but not for method 2 (inset of Figure 4B). The 99% confidence bands denote the region that contains the true fit of the data. The nonoverlapping confidence bands in LAD fitting show that the LAD fitting is more precise than the Gaussian fitting (and see below for a brief explanation).

Using method 1, we obtain for junctions with SAM_{even} $\log_{10}|J_0|_{even} = 2.70 \pm 0.23$ A/cm^2 and $\beta_{even} = 1.05 \pm 0.04$ n_C^{-1}, and for junctions with SAM_{odd} $\log_{10}|J_0|_{odd} = 2.54 \pm 0.17$ A/cm^2 and $\beta_{odd} = 1.13 \pm 0.03$ n_C^{-1}. (The error bars represent 99% confidence levels fitted from values of $\langle \log_{10}|J| \rangle_G$). Using method 2, we obtained $\log_{10}|J_0|_{even} = 2.72 \pm 0.03$ A/cm^2 and $\beta_{even} = 1.05 \pm 0.01$ n_C^{-1}, and $\log_{10}|J_0|_{odd} = 2.53 \pm 0.03$ A/cm^2 and $\beta_{odd} = 1.12 \pm 0.01$ n_C^{-1} (here the error represents the 99% confidence levels; Table 1). We calculated the probability (p values) by student Z-test to determine the statistical significance of the odd−even effects in the values of J_0 and β.[48] The null hypothesis that $\log_{10}|J_0|_{odd} = \log_{10}|J_0|_{even}$ and $\beta_{odd} = \beta_{even}$ is rejected ($p < 0.01$) for method 2, but not for method 1. The p values are consistent with the overlapping confidence band in Gaussian (Figure 4A, inset) and nonoverlapping confidence band in LAD fitting (Figure 4B, inset). The LAD fitting procedure is more precise in determining the odd−even effect, as in this analysis all data are taken into consideration; i.e., eq 1 is fitted to all data ($N_{even} = 2700$ and $N_{odd} = 2400$), while, in method 1, eq 1 is only fitted to the values of $\langle \log_{10}|J| \rangle_G$. The number of data points is only $N_{even} = 9$ or $N_{odd} = 8$. As argued by Reus et al.,[48] both statistical methods give reasonably precise values of $\log_{10}|J_0|$ and β, but method 2 is about an order of magnitude more precise than method 1. See ref 46 for a more detailed discussion regarding the differences in precision and accuracy of both methods.

Origin of the Odd−Even Effect. In the previous section we showed that the odd−even effect manifests itself in both the values of $\log_{10}|J_0|$ and β, but as mentioned in the introduction, DC methods only measure the total currents impeded by all components of the junctions. To determine how the different components of the junctions impede the flow of charges across the junctions, and how each of these components is influenced by odd−even effects quantitatively, we studied the junctions by impedance spectroscopy using junctions that had their J(V) characteristics within one log-standard deviation of the log-mean value of J. We measured the frequency response to a sinusoidal perturbation with an amplitude of 30 mV around zero bias with a frequency ranging from 1 Hz to 1 MHz.

Figure 5 shows the Bode and phase plots of $Ag^{A\text{-}TS}$-SC_n//GaO_x/EGaIn junctions with $n = 6$ to 18. The Nyquist plots (Figure S1) show one semicircle for all junctions indicating the presence of only one capacitor. The modulus of complex impedance $|Z|$ is constant at low frequencies and is dominated by the R_{SAM} (Figure 5A and C). The $|Z|$ starts to decrease with increasing frequency for frequencies higher than the so-called transition frequency (f_T), which is defined as the frequency when the $|Z|$ drops 10%, when capacitive effects dominate.[65] The f_T decreases with the R_{SAM} and was not accurately

DOI: 10.1021/jacs.5b05761
J. Am. Chem. Soc. 2015, 137, 10659−10667

Table 1. Electrical Properties of $Ag^{A\text{-}TS}$-SC_n//GaO_x/EGaIn Junctions in DC and AC Measurements

	DC (Gaussian)		DC (LAD)		AC	
surfaces	log| J_0| (A/cm^2)	β (n_C^{-1})	log| J_0| (A/cm^2)	β (n_C^{-1})	R_0 (Ω·cm^2)	β (n_C^{-1})
odd	2.54 ± 0.17	1.13 ± 0.03	2.53 ± 0.03	1.12 ± 0.01	(4.04 ± 0.20) × 10^{-3}	1.02 ± 0.06
even	2.70 ± 0.23	1.05 ± 0.04	2.72 ± 0.03	1.05 ± 0.01	(9.46 ± 0.13) × 10^{-4}	1.04 ± 0.03

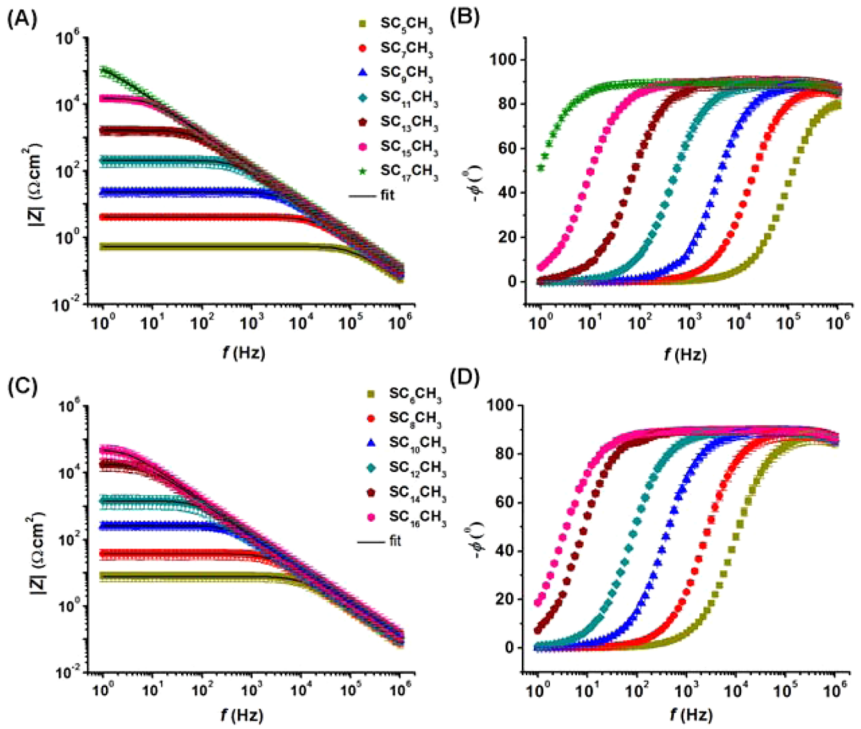

Figure 5. Bode (A, C) and phase (B, D) plots for the $Ag^{A\text{-}TS}$-SC_n//GaO_x/EGaIn junctions with n = 6, 8, 10, 12, 14, 16, or 18 (A, B), and n = 7, 9, 11, 13, 15, or 17 (C, D), respectively.

measurable for junctions with $n < 6$. As mentioned above, the junction size (the geometrical contact area A_{geo} was 9.6 × 10^2 μm^2) was chosen such that the capacitance could be measured reliably (the instrumental limit is ~1 pF) without affecting the quality of the junctions (very large contact areas, $A_{geo} > 9.6 \times 10^2$ μm^2, result in leakage currents).[35] These observations are consistent with an equivalent circuit shown in Figure 1b. The value of R_c is dominated by the SAM//GaO_x resistance ($R_{c,t}$), and we reported before that the contact resistances of the contact probes with the electrodes, the low resistance of the GaO_x layer (3.3−5.8 × 10^{-4} Ω·cm^2),[29,49] or the Ag-thiolate interface only adds about 2% to the measured value R_c.[29] Therefore, we assume in the discussion below that $R_c \approx R_{c,t}$.

The physical meaning of the circuit elements can be understood by the Landauer formalism that includes the contact resistance given in eq 2 as described elsewhere[66] (see Background). The first term of this equation shows that the value of R_c should equal to $1/G_0$ (assuming M = 1 and ideal point contact), but in our junctions R_c is typically 10^{-2} to 10^{-3} G_0 which implies that the SAM—electrode contact is, as expected, not ideal and that scattering (reflections) across the interfaces (including the GaO_x layer) is important. The R_{SAM} values are on the same order as those measured in Au-SC_n//Au where the top electrode is a conductive probe AFM tip.[38] The value of R_{SAM} is determined by the properties of the SAM and the electrode materials and the SAM—electrode interactions as given by the second term of eq 2.

Before we analyzed the data, we used the Kramers−Kronig (KK) test to validate the linearity and stability of our data. Figure S3 shows the KK plots, and the low χ_{KK}^2 values (6 × 10^{-4} to 2 × 10^{-3}; Table S3) confirm the stability and linearity of our system with acceptable signal-to-noise ratios. To extract the values of R_{SAM}, C_{SAM}, and R_c, the complex impedance was modeled using the equivalent circuit shown in Figure 1B for which Z is given by eq 4 where ω (= $2\pi f$) is the varying frequency in rad/s.[67] The residual plots for nonlinear least-squares fitting of the equivalent circuit to the data are shown in Figure S4. The χ_{fit}^2 values are similar in value to the χ_{KK}^2 values (Table S3) from which we conclude that the data fitted well within the experimental error.

$$Z = \left(R_c + \frac{R_{SAM}}{1 + \omega^2 R_{SAM}^2 C_{SAM}^2}\right) - j\left(\frac{\omega C_{SAM} R_{SAM}^2}{1 + \omega^2 R_{SAM}^2 C_{SAM}^2}\right) \quad (4)$$

Figure 6A shows the value of R_{SAM} and R_c as a function of n_C (the fitting results are listed in Table S4). The error bars represent the standard deviations of three different junctions on different substrates. The odd−even effect in the value of R_c is small but significant (inset of Figure 6A). The values of R_{SAM} also follow an odd−even effect, and the absolute values of R_{SAM} are orders of magnitude larger than the values of R_c. Extrapolation of the data implies that R_c could only, if ever, dominate over R_{SAM} for junctions with $n \leq 2$. These results show that the odd−even effect observed in DC measurements

DOI: 10.1021/jacs.5b05761
J. Am. Chem. Soc. 2015, 137, 10659−10667

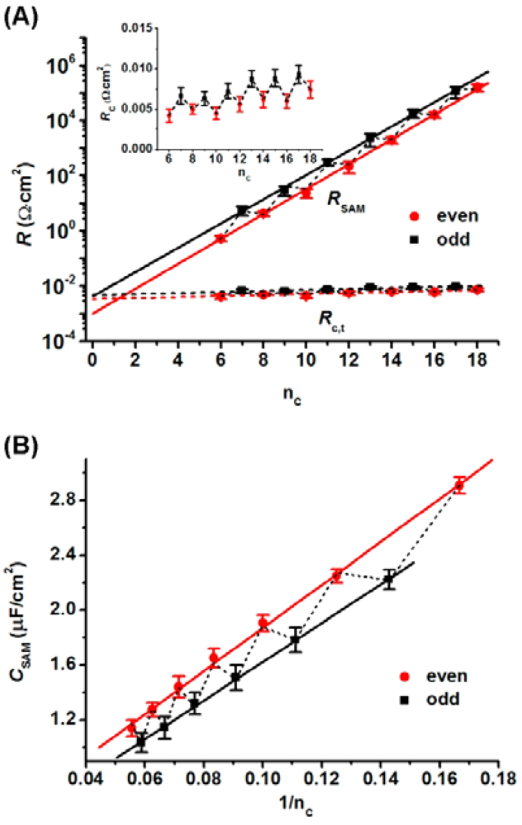

Figure 6. (A) Semilog plots of the SAM resistance (R_{SAM}; the solid lines are fits to eqs 5 and 6) and SAM—top contact resistance ($R_{c,t}$) against n (inset: R_c as a function of n with linear scales). (B) The SAM capacitance (C_{SAM}; the solid lines are fits to eqs 7 and 8) as a function of n. The dashed lines are guides to the eye.

cannot be caused by the SAM−electrode interfaces because $R_{SAM} \gg R_{c,t}$.

The general tunnel equation can be rewritten in terms of R_{SAM} to give

$$R_{SAM,odd} = R_{SAM,odd,0}e^{\beta_{odd}d} \quad (5)$$

$$R_{SAM,even} = R_{SAM,even,0}e^{\beta_{even}d} \quad (6)$$

We plotted R_{SAM} as a function of n_C to which we fitted eqs 5 and 6 (Figure 6A) and obtained β_{odd} = 1.02 ± 0.06 n_C^{-1} and $R_{SAM,odd,0}$ = (4.04 ± 0.20) × 10^{-3} Ω·cm², and β_{even} = 1.04 ± 0.03 n_C^{-1} and $R_{SAM,even,0}$ = (9.46 ± 0.13) × 10^{-4} Ω·cm² (the error represents the 99% confidence levels; Table 1). These values of β_{odd} and β_{even} are statistically indistinguishable (very similar to the β_{odd} and β_{even} extracted from the DC data described above), but the odd−even effect in R_{SAM} is obvious and statistically significant. From these observations we conclude odd SAMs impede charge transport more than even SAMs. This odd−even effect is also reflected in the fitting parameter $R_{SAM,0}$ ($R_{SAM,odd,0}$ = is a factor of ∼5 larger than $R_{SAM,even,0}$).

Figure 6B shows the odd−even effect in C_{SAM} as a function of $1/n_C$. The capacitance of a parallel plate capacitor is proportional to the geometrical contact area and inversely proportional to the distance d_{SAM} between the two parts and is given by eqs 7 and 8 with ε_0 as the permittivity of free space (≈ 8.854 × 10^{-12} F/m), $\varepsilon_{r,SAM}$ as the dielectric constant of the SAMs, and A_{geo} as the geometric contact area of junctions.

$$C_{SAM,odd} = \varepsilon_0\varepsilon_{r,odd}A_{geo}/d_{SAM} \quad (7)$$

$$C_{SAM,even} = \varepsilon_0\varepsilon_{r,even}A_{geo}/d_{SAM} \quad (8)$$

By fitting eqs 7 and 8 to the plots of C_{SAM} vs $1/d_{SAM}$, we obtained the values of $\varepsilon_{r,SAM}$. We found a value of $\varepsilon_{r,even}$ of 3.52 ± 0.20, and for junctions with n_{odd}, the value of $\varepsilon_{r,odd}$ is 3.11 ± 0.12 (the error bars represent the standard deviations of three individual experiments). These values are comparable to previously reported data.[29,68] Based on the effective thickness of the SAMs, d_{cal}, estimated using CPK models and the small tilt angle for SAMs of Ag of 11° (Table S5), only a weak odd−even effect was observed when we plotted the estimated C_{SAM} using the experimentally determined $\varepsilon_{r,SAM}$ values and eqs 7 and 8 (Figure S2). We argue that the small odd−even effect in the effective thickness of the SAM cannot explain the experimentally observed large odd−even effects in C_{SAM} (or R_{SAM}). Therefore, we believe that the odd−even effect in the value of C_{SAM} originates from the intrinsic properties of the SAMs. Our results also imply that the parallel plate approximation is limited and is useful in qualitative discussions, but an improved theory is required to understand all details (see for example recent work by Ratner et al.[56]) which is outside the scope of the present work.

CONCLUSIONS

The odd−even effect is a property of the junctions. We examined the origin of the odd−even effect in the value of J observed in DC measurements across $Ag^{A\text{-}TS}$-$SC_{n-1}CH_3$//GaO_x/EGaIn junctions. We used a statistically robust J(V) data set (a large number of J(V) curves (N_{tot} = 5100) and a broad range of n values of 2−18) to confirm that the odd−even effects in the values of J_0 and β (obtained by a simplified version of the Simmons equation) are statistically significant ($p < 10^{-5}$). Although the values of J_0 and β are often related to the SAM—electrode interfaces and the molecular component of the junctions, respectively, their physical meaning is not clear. To address the question whether the odd−even effect is an interface effect (i.e., the contact resistance as defined in eq 2) or not, we investigated the electrical properties of the junctions by impedance spectroscopy. This method allowed us to investigate the components of the junctions that impede charge transport directly (the SAM resistance (R_{SAM}), the SAM capacitance (C_{sAM}), and the SAM—top electrode contact resistance (R_c)). Odd−even effects are apparent in *each* component.

Origins of the Odd−Even Effects. Our results indicate that (at least) three different types of odd−even effects (in the values of R_{SAM}, C_{SAM}, and R_c) cause the odd−even effect in the measured values of J in J(V) measurements. To explain the origin(s) of these odd even effects, we note that SAM-based junctions have to be treated as a single physical organic system composed to two molecule−electrode interfaces and the SAM: a change in one of these components will affect all other components. For instance, a change in the molecule—electrode binding will cause a change in the tunneling barrier height and the transmission probability T (note: without necessarily changing the contact resistance provided, the number of transverse modes M remains constant; eq 2). Therefore, distinguishing interface effects from molecular effects is not useful, as the junction should be treated as a single physical−organic system, but one can distinguish between the contact resistance and the resistance of the tunnel junction as defined in eq 2.

DOI: 10.1021/jacs.5b05761
J. Am. Chem. Soc. 2015, 137, 10659−10667

Origin of the Odd–Even Effect in the Contact Resistance. Since $R_{SAM} \gg R_c$, the odd–even effect in the values of J determined by DC methods (i.e., J(V) measurements) does *not* originate from the SAM—electrode contact resistances. The odd–even effect in R_c is small but significant when measured by impedance spectroscopy. The reason for this odd–even effect could be that the number of transverse mode M changes (as the shape of the tunneling barrier changes; see below) or that scattering effects change (perhaps as a result of an odd–even effect in the wetting behavior of GaO_x/EGaIn with the SAM).

Origin of the Odd–Even Effect in the SAM Resistance and Capacitance. Although our study reveals that the odd–even effects originate from the SAMs, it does not explain why charges are more impeded by odd SAMs than even SAMs. Dubi[61] proposed that odd–even effects arise from molecule–molecule coupling inside the SAMs and predicted the magnitude of the odd–even effect would decrease with increasing n. Zhang et al.[62] showed theoretically an odd–even effect in the hybridization of the molecular orbitals with the top electrode resulting in an odd–even effect in the shape of the tunneling barrier and predicted that the odd–even effect would be prominent for $10 < n < 19$.

Our data show that the odd–even effect is apparent for n = 2–18 and that the odd–even effect in the magnitude J (determined by J(V)) measurements increases with increasing n. This observation is against the prediction by Dubi and indicates that molecule–molecule interactions play a minor role as, perhaps, can be expected from the relative small change in the van der Waals packing energy.[61] Cahen et al.[23] suggested that molecule–molecule interactions are important in the odd–even effect in J observed in Si-SC_nPh//Pd junctions. In these junctions π–π interactions between the Ph groups follow an odd–even effect which, in turn, causes a change in the tunneling barrier height and hence seems to agree with the prediction by Dubi.

Laibinis et al.[34,46,69] showed that odd and even SAMs pack differently and have different twist angles γ which were taken into consideration in the calculations by Zhang et al.[62] These authors showed that the interaction of the distal hydrogen with the top electrode follows an odd–even effect because of an odd–even effect in γ. The authors found that the evens interact with the top electrode more strongly than odds which lowers the tunneling barrier height and increases the tunneling rate. We favor this explanation for two reasons. (i) The odd–even effect in the orientation in the terminal CH_2CH_3 group is on Ag likely too small to cause a measurable odd–even effect due to the small tilt angle of the SAM. (ii) The odd–even effect in the dielectric constant of the SAM is large ($\varepsilon_{r,even} = 3.52 \pm 0.20$ and $\varepsilon_{r,odd} = 3.11 \pm 0.12$) which indicates that these odd and even SAMs pack differently which is in agreement with the odd–even effect in γ.

Factors That Are Unlikely to Contribute to the Odd–Even Effect. We believe that the following three factors that could potentially cause odd–even effects in the measured J(V) data across Ag^{TS}-SC_n//GaO_x/EGaIn junctions are not important. (i) Considering the very weak dipole moments associated with the alkyl chains (in all of our junctions the surface dipole is dominated by the Ag–S contact), we do not believe that an odd–even effect in dipole is important unlike in junctions with, for instance, SAMs with phenyl head groups.[23] (ii) Differences in the effective barrier width of the SC_n SAMs (as a result of an odd–even effect in the effective length of the SAM) or barrier height (as a result of an odd–even effect in the SAM packing energies) are too small to cause a measurable odd–even effect unlike in junctions with, with, for instance, SAMs with large terminal Fc groups.[70] (iii) Odd–even effects in the wetting of SC_n SAMs by water have been reported before,[2,71,72] but we rule out the potential difference in wetting behavior of the GaO_x/EGaIn with the SAM as a cause of the odd–even effect observed in DC measurements (though it could be the cause of the small odd–even effect in the SAM—electrode contact resistance observed by AC measurements).

We believe that the results described here will help guide future experimental and theoretical investigations to address the question why odds impede charge transfer more than evens in these junctions, in more detail. In addition, Ratner et al.[56] showed theoretically that SAMs are promising for applications in high-capacitance dielectrics and that subtle changes in the structure of the SAMs may have a profound effect in the dielectric properties of the SAMs. Our experimental results show that, indeed, the odd–even effects in the dielectric properties of the junctions are induced by the SAMs and that it is possible to tune the dielectric properties of SAM-based junctions at the molecular level.

■ ASSOCIATED CONTENT

Supporting Information

The Supporting Information is available free of charge on the ACS Publications website at DOI: 10.1021/jacs.5b05761.

Experimental details, electrical characterization of the junctions, KK-plots, the residual plots, and χ^2 values (PDF)

■ AUTHOR INFORMATION

Corresponding Author

*christian.nijhuis@nus.edu.sg

Notes

The authors declare no competing financial interest.

■ ACKNOWLEDGMENTS

The Singapore National Research Foundation (NRF Award No. NRF-RF 2010-03 to C.A.N.). Prime Minister's Office, Singapore under its Medium sized centre program is kindly acknowledged for supporting this research. We also would like to thank Damien Thompson and Enrique Del Barco for the very insightful discussions.

■ REFERENCES

(1) Eckermann, A. L.; Feld, D. J.; Shaw, J. A.; Meade, T. J. *Coord. Chem. Rev.* **2010**, *254*, 1769.
(2) Tao, F.; Bernasek, S. L. *Chem. Rev.* **2007**, *107*, 1408.
(3) Nijhuis, C. A.; Huskens, J.; Reinhoudt, D. N. *J. Am. Chem. Soc.* **2004**, *126*, 12266.
(4) Bissell, R. A.; Cordova, E.; Kaifer, A. E.; Stoddart, J. F. *Nature* **1994**, *369*, 133.
(5) Freund, H. J.; Nilius, N.; Risse, T.; Schauermann, S. *Phys. Chem. Chem. Phys.* **2014**, *16*, 8148.
(6) Youngblood, W. J.; Lee, S. H. A.; Maeda, K.; Mallouk, T. E. *Acc. Chem. Res.* **2009**, *42*, 1966.
(7) Ma, W.; Long, Y. T. *Chem. Soc. Rev.* **2014**, *43*, 30.
(8) Beratan, D. N.; Skourtis, S. S.; Balabin, I. A.; Balaeff, A.; Keinan, S.; Venkatramani, R.; Xiao, D. Q. *Acc. Chem. Res.* **2009**, *42*, 1669.
(9) Gohler, B.; Hamelbeck, V.; Markus, T. Z.; Kettner, M.; Hanne, G. F.; Vager, Z.; Naaman, R.; Zacharias, H. *Science* **2011**, *331*, 894.

DOI: 10.1021/jacs.5b05761
J. Am. Chem. Soc. 2015, 137, 10659–10667

(10) Liu, Y.; Yuan, L.; Yang, M.; Zheng, Y.; Li, L.; Gao, L.; Nerngchamnong, N.; Nai, C. T.; Sangeeth, C. S.; Feng, Y. P.; Nijhuis, C. A.; Loh, K. P. *Nat. Commun.* **2014**, *5*, 5461.
(11) Darwish, N.; Aragonès, A. C.; Darwish, T.; Ciampi, S.; Díez-Pérez, I. *Nano Lett.* **2014**, *14*, 7064.
(12) Fracasso, D.; Muglali, M. I.; Rohwerder, M.; Terfort, A.; Chiechi, R. C. *J. Phys. Chem. C* **2013**, *117*, 11367.
(13) Mirjani, F.; Thijssen, J. M.; Whitesides, G. M.; Ratner, M. A. *ACS Nano* **2014**, *8*, 12428.
(14) Huang, C. C.; Rudnev, A. V.; Hong, W. J.; Wandlowski, T. *Chem. Soc. Rev.* **2015**, *44*, 889.
(15) Díez-Pérez, I.; Hihath, J.; Lee, Y.; Yu, L. P.; Adamska, L.; Kozhushner, M. A.; Oleynik, II; Tao, N. J. *Nat. Chem.* **2009**, *1*, 635.
(16) McCreery, R. L.; Bergren, A. J. *Adv. Mater.* **2009**, *21*, 4303.
(17) Akkerman, H. B.; de Boer, B. *J. Phys.: Condens. Matter* **2008**, *20*, 013001.
(18) Bergfield, J. P.; Ratner, M. A. *Phys. Status Solidi B* **2013**, *250*, 2249.
(19) McCreery, R. L. *Chem. Mater.* **2004**, *16*, 4477.
(20) Guo, S. Y.; Hihath, J.; Díez-Pérez, I.; Tao, N. J. *J. Am. Chem. Soc.* **2011**, *133*, 19189.
(21) Luo, L.; Balhorn, L.; Vlaisavljevich, B.; Ma, D. X.; Gagliardi, L.; Frisbie, C. D. *J. Phys. Chem. C* **2014**, *118*, 26485.
(22) Perrin, M. L.; Frisenda, R.; Koole, M.; Seldenthuis, J. S.; Gil, J. A. C.; Valkenier, H.; Hummelen, J. C.; Renaud, N.; Grozema, F. C.; Thijssen, J. M.; Dulic, D.; van der Zant, H. S. J. *Nat. Nanotechnol.* **2014**, *9*, 830.
(23) Toledano, T.; Sazan, H.; Mukhopadhyay, S.; Alon, H.; Lerman, K.; Bendikov, T.; Major, D. T.; Sukenik, C. N.; Vilan, A.; Cahen, D. *Langmuir* **2014**, *30*, 13596.
(24) Salomon, A.; Cahen, D.; Lindsay, S.; Tomfohr, J.; Engelkes, V. B.; Frisbie, C. D. *Adv. Mater.* **2003**, *15*, 1881.
(25) Yuan, L.; Jiang, L.; Thompson, D.; Nijhuis, C. A. *J. Am. Chem. Soc.* **2014**, *136*, 6554.
(26) Yuan, L.; Jiang, L.; Zhang, B.; Nijhuis, C. A. *Angew. Chem., Int. Ed.* **2014**, *53*, 3377.
(27) Vilan, A. *J. Phys. Chem. C* **2007**, *111*, 4431.
(28) Wang, G.; Kim, T. W.; Lee, T. *J. Mater. Chem.* **2011**, *21*, 18117.
(29) Sangeeth, C. S. S.; Wan, A.; Nijhuis, C. A. *J. Am. Chem. Soc.* **2014**, *136*, 11134.
(30) Akkerman, H. B.; Naber, R. C. G.; Jongbloed, B.; van Hal, P. A.; Blom, P. W. M.; de Leeuw, D. M.; de Boer, B. *Proc. Natl. Acad. Sci. U. S. A.* **2007**, *104*, 11161.
(31) Stoliar, P.; Kshirsagar, R.; Massi, M.; Annibale, P.; Albonetti, C.; de Leeuw, D. M.; Biscarini, F. *J. Am. Chem. Soc.* **2007**, *129*, 6477.
(32) Thuo, M. M.; Reus, W. F.; Nijhuis, C. A.; Barber, J. R.; Kim, C.; Schulz, M. D.; Whitesides, G. M. *J. Am. Chem. Soc.* **2011**, *133*, 2962.
(33) Nerngchamnong, N.; Yuan, L.; Qi, D. C.; Li, J.; Thompson, D.; Nijhuis, C. A. *Nat. Nanotechnol.* **2013**, *8*, 113.
(34) Baghbanzadeh, M.; Simeone, F. C.; Bowers, C. M.; Liao, K. C.; Thuo, M.; Baghbanzadeh, M.; Miller, M. S.; Carmichael, T. B.; Whitesides, G. M. *J. Am. Chem. Soc.* **2014**, *136*, 16919.
(35) Jiang, L.; Sangeeth, C. S. S.; Wan, A.; Vilan, A.; Nijhuis, C. A. *J. Phys. Chem. C* **2015**, *119*, 960.
(36) Vilan, A.; Cahen, D.; Kraisler, E. *ACS Nano* **2013**, *7*, 695.
(37) Beebe, J. M.; Engelkes, V. B.; Miller, L. L.; Frisbie, C. D. *J. Am. Chem. Soc.* **2002**, *124*, 11268.
(38) Engelkes, V. B.; Beebe, J. M.; Frisbie, C. D. *J. Am. Chem. Soc.* **2004**, *126*, 14287.
(39) Kim, B.; Choi, S. H.; Zhu, X. Y.; Frisbie, C. D. *J. Am. Chem. Soc.* **2011**, *133*, 19864.
(40) Shpaisman, H.; Seitz, O.; Yaffe, O.; Roodenko, K.; Scheres, L.; Zuilhof, H.; Chabal, Y. J.; Sueyoshi, T.; Kera, S.; Ueno, N.; Vilan, A.; Cahen, D. *Chem. Sci.* **2012**, *3*, 851.
(41) York, R. L.; Nguyen, P. T.; Slowinski, K. *J. Am. Chem. Soc.* **2003**, *125*, 5948.
(42) Wang, G.; Kim, Y.; Choe, M.; Kim, T. W.; Lee, T. *Adv. Mater.* **2011**, *23*, 755.
(43) Bonifas, A. P.; McCreery, R. L. *Nat. Nanotechnol.* **2010**, *5*, 612.
(44) Reus, W. F.; Thuo, M. M.; Shapiro, N. D.; Nijhuis, C. A.; Whitesides, G. M. *ACS Nano* **2012**, *6*, 4806.
(45) Cademartiri, L.; Thuo, M. M.; Nijhuis, C. A.; Reus, W. F.; Tricard, S.; Barber, J. R.; Sodhi, R. N. S.; Brodersen, P.; Kim, C.; Chiechi, R. C.; Whitesides, G. M. *J. Phys. Chem. C* **2012**, *116*, 10848.
(46) Laibinis, P. E.; Whitesides, G. M.; Allara, D. L.; Tao, Y. T.; Parikh, A. N.; Nuzzo, R. G. *J. Am. Chem. Soc.* **1991**, *113*, 7152.
(47) Weiss, E. A.; Kaufman, G. K.; Kriebel, J. K.; Li, Z.; Schalek, R.; Whitesides, G. M. *Langmuir* **2007**, *23*, 9686.
(48) Reus, W. F.; Nijhuis, C. A.; Barber, J. R.; Thuo, M. M.; Tricard, S.; Whitesides, G. M. *J. Phys. Chem. C* **2012**, *116*, 6714.
(49) Simeone, F. C.; Yoon, H. J.; Thuo, M. M.; Barber, J. R.; Smith, B.; Whitesides, G. M. *J. Am. Chem. Soc.* **2013**, *135*, 18131.
(50) Wan, A.; Jiang, L.; Sangeeth, C. S. S.; Nijhuis, C. A. *Adv. Funct. Mater.* **2014**, *24*, 4442.
(51) Jiang, L.; Wang, T.; Nijhuis, C. A. *Thin Solid Films*, submitted.
(52) Liu, D. Q.; He, Z. K.; Su, Y. R.; Diao, Y.; Mannsfeld, S. C. B.; Bao, Z. A.; Xu, J. B.; Miao, Q. *Adv. Mater.* **2014**, *26*, 7190.
(53) Zaccari, I.; Catchpole, B. G.; Laurenson, S. X.; Davies, A. G.; Walti, C. *Langmuir* **2014**, *30*, 1321.
(54) Acton, B. O.; Ting, G. G.; Shamberger, P. J.; Ohuchi, F. S.; Ma, H.; Jen, A. K. Y. *ACS Appl. Mater. Interfaces* **2010**, *2*, 511.
(55) Sun, Y. T.; Krishtab, M.; Struyf, H.; Verdonck, P.; De Feyter, S.; Baklanov, M. R.; Armini, S. *Langmuir* **2014**, *30*, 3832.
(56) Heitzer, H. M.; Marks, T. J.; Ratner, M. A. *ACS Nano* **2014**, *8*, 12587.
(57) Datta, S. *Electronic transport in mesoscopic systems*; Cambridge University Press: Cambridge, U.K., 1995.
(58) Bowers, C. M.; Liao, K. C.; Zaba, T.; Rappoport, D.; Baghbanzadeh, M.; Breiten, B.; Krzykawska, A.; Cyganik, P.; Whitesides, G. M. *ACS Nano* **2015**, *9*, 1471.
(59) Liao, K. C.; Bowers, C. M.; Yoon, H. J.; Whitesides, G. M. *J. Am. Chem. Soc.* **2015**, *137*, 3852.
(60) Yuan, L.; Thompson, D.; Nerngchamnong, N.; Liang, C.; Nijhuis, C. A. *J. Phys. Chem. C* **2015**, *119*, 17910.
(61) Dubi, Y. *J. Phys. Chem. C* **2014**, *118*, 21119.
(62) Nurbawono, A.; Liu, S. L.; Nijhuis, C. A.; Zhang, C. *J. Phys. Chem. C* **2015**, *119*, 5657.
(63) Nerngchamnong, N.; Wu, H.; Sotthewes, K.; Yuan, L.; Cao, L.; Roemer, M.; Lu, J.; Loh, K. P.; Troadec, C.; Zandvliet, H. J.; Nijhuis, C. A. *Langmuir* **2014**, *30*, 13447.
(64) Jiang, L.; Yuan, L.; Cao, L.; Nijhuis, C. A. *J. Am. Chem. Soc.* **2014**, *136*, 1982.
(65) Sangeeth, C. S. S.; Jaiswal, M.; Menon, R. *J. Phys.: Condens. Matter* **2009**, *21*, 072101.
(66) Sangeeth, C. S. S.; Wan, A.; Nijhuis, C. A. *Nanoscale* **2015**, *7*, 12061.
(67) Barsoukov, E., Macdonald, J. R., Eds.; *Impedance Spectroscopy: Theory, Experiment, and Applications*, 2nd ed.; John Wiley & Sons, Inc.: Hoboken, NJ, USA, 2005.
(68) Rampi, M. A.; Schueller, O. J. A.; Whitesides, G. M. *Appl. Phys. Lett.* **1998**, *72*, 1781.
(69) Love, J. C.; Estroff, L. A.; Kriebel, J. K.; Nuzzo, R. G.; Whitesides, G. M. *Chem. Rev.* **2005**, *105*, 1103.
(70) Wang, Y.; Canchaya, J. G. S.; Dong, W.; Alcami, M.; Busnengo, H. F.; Martin, F. *J. Phys. Chem. A* **2014**, *118*, 4138.
(71) Lee, S.; Puck, A.; Graupe, M.; Colorado, R.; Shon, Y. S.; Lee, T. R.; Perry, S. S. *Langmuir* **2001**, *17*, 7364.
(72) Newcomb, L. B.; Tevis, I. D.; Atkinson, M. B. J.; Gathiaka, S. M.; Luna, R. E.; Thuo, M. *Langmuir* **2014**, *30*, 11985.

DOI: 10.1021/jacs.5b05761
J. Am. Chem. Soc. 2015, 137, 10659−10667